Isotope and multiband effects in layered superconductors

2012 J. Phys.: Condens. Matter 24 233201

(http://iopscience.iop.org/0953-8984/24/23/233201)

J. Phys.: Condens. Matter **24** (2012) 233201 (13pp) doi:10.1088/0953-8984/24/23/233201

TOPICAL REVIEW

Isotope and multiband effects in layered superconductors

Annette Bussmann-Holder[1] **and Hugo Keller**[2]

[1] Max-Planck-Institut für Festkörperforschung, Heisenbergstrasse 1, D-70569 Stuttgart, Germany
[2] Physik Institut der Universität Zürich, Winterthurerstrasse 190, CH-8057 Zürich, Switzerland

E-mail: keller@physik.uzh.ch

Received 21 October 2011, in final form 27 February 2012
Published 4 May 2012
Online at stacks.iop.org/JPhysCM/24/233201

Abstract
In this review we consider three classes of superconductors, namely cuprate superconductors, MgB_2 and the new Fe based superconductors. All of these three systems are layered materials and multiband compounds. Their pairing mechanisms are under discussion with the exception of MgB_2, which is widely accepted to be a 'conventional' electron–phonon interaction mediated superconductor, but extending the Bardeen–Cooper–Schrieffer (BCS) theory to account for multiband effects. Cuprates and Fe based superconductors have higher superconducting transition temperatures and more complex structures. Superconductivity is doping dependent in these material classes unlike in MgB_2 which, as a pure compound, has the highest values of T_c and a rapid suppression of superconductivity with doping takes place. In all three material classes isotope effects have been observed, including exotic ones in the cuprates, and controversial ones in the Fe based materials. Before the area of high-temperature superconductivity, isotope effects on T_c were the signature for phonon mediated superconductivity—even when deviations from the BCS value to smaller values were observed. Since the discovery of high T_c materials this is no longer evident since competing mechanisms might exist and other mediating pairing interactions are discussed which are of purely electronic origin. In this work we will compare the three different material classes and especially discuss the experimentally observed isotope effects of all three systems and present a rather general analysis of them. Furthermore, we will concentrate on multiband signatures which are not generally accepted in cuprates even though they are manifest in various experiments, the evidence for those in MgB_2, and indications for them in the Fe based compounds. Mostly we will consider experimental data, but when possible also discuss theoretical models which are suited to explain the data.

(Some figures may appear in colour only in the online journal)

Contents

1. Introduction

The discovery of high T_c superconductivity (HTS) in copper oxide compounds [1] was motivated by the idea

that the conventional Bardeen–Cooper–Schrieffer (BCS) phonon mediated pairing glue is insufficient to exceed superconducting transition temperatures $T_c > 30$ K. The strong coupling Eliashberg formulation of the BCS theory shows that the phonon energy is inversely related to the coupling constant, which implies that a large coupling as required for large values of T_c inevitably leads to a structural instability. Bednorz and Müller were inspired by the work of Höck *et al* [2], who demonstrated that strong electron lattice coupling does not necessarily induce a lattice instability but can support a Jahn–Teller polaron. A prerequisite for the existence of this quasi-particle is the degeneracy of electronic states which can be lifted through the coupling to the lattice and lower the ground state energy as long as the induced strain energy remains small. In addition, an almost insulating behavior is needed where the resistivity as a function of temperature shows an upturn due to polaron induced localization [3]. As such their search for HTS started with perovskite type oxides, where a transition metal is surrounded by an octahedron of oxygen ions. The distortion of the oxygen ion framework can then cause a lifting of the electronic degeneracy of the transition metal ion. From previous work they knew that Cu is one of the strongest Jahn–Teller ions [4], and after various failures in their search for HTS [3] they succeeded in breaking the 30 K limit with the discovery of HTS in $La_{2-x}Ba_xCuO_4$ [1]. Very rapidly after this breakthrough the hitherto maximum value of $T_c = 160$ K was reached under pressure [5].

In spite of the background idea of Bednorz and Müller about the pairing glue in terms of polarons, the antiferromagnetic properties of the parent compounds have motivated many researchers to explain HTS in terms of purely electronic models. This is mainly based on the fact that the undoped cuprates are half filled band systems which should be metals but are in fact insulators. To understand this paradigm, a large onsite Coulomb repulsion at the copper ion site has to be invoked which inhibits double occupancy and metallic properties. This large Hubbard U in turn can explain the antiferromagnetism and also sets the largest energy scale in the physics of HTS. It might, however, hide crucial and important smaller energy scales as given by polaron formation for example.

The issue about the pairing mechanism in cuprates still remains a matter of debate more than 25 years after their discovery. Yet it should be noted that purely electronic models are based on a homogeneous approach, they do not cover isotope effects and also ignore local lattice responses. As such they are at least incomplete, as will be shown here, where some important aspects of unconventional isotope effects and multi-component superconductivity in cuprates will be discussed.

The discovery of MgB_2 [6] has raised the interest in HTS again. In particular its layered structure, where conducting sheets are intercalated by insulating layers, has provided some evidence for commonalities with cuprates. For this material it soon became obvious that the pairing is most likely phonon mediated [7]. Different from conventional BCS superconductors, various experiments provided clear evidence that two kinds of carriers participate in the pairing mechanism, namely σ- and π-electrons [8–10]. This multiband effect gives rise to largely enhanced values of T_c, as predicted early on [9–11]. Quite opposite to cuprates and Fe based compounds, doping is not supporting superconductivity but is always detrimental. Only the pure compound shows the highest values of T_c and any doping leads to a rather rapid decrease in it.

Fe based superconductors, only discovered in 2008 [12], were first believed to break the record T_cs of cuprates. Until now, however, T_c remains below the liquid nitrogen temperature [13], leaving the record position of cuprates untouched. Analogous to cuprates is their phase diagram, where undoped compounds show antiferromagnetism [14–16]. This is rapidly destroyed by doping and superconductivity either partially coexists with it [17, 18] or appears only when the magnetism is completely suppressed. In this respect their phase diagrams carry some similarities to cuprates. On the other hand Fe based superconductors are metallic in the undoped case whereas cuprates are insulating, suggesting that the former are less strongly correlated [19].

It also seems that Fe based superconductors are not strongly correlated, since their metallic properties are rather conventional Fermi liquid like. Isotope effects have been investigated for only a very few systems, with controversial results [20–22]. Unlike cuprates, experiments in Fe based materials are largely hampered since isotope exchange is not possible *in situ* and samples have to be grown with different isotopes under the same growth conditions [22]. Rather analogous to cuprates, strong correlations with local structural distortions have been seen and seem to correlate with T_c.

The three material classes of high-temperature superconductors (HTSCs) will be discussed from the above mentioned limited perspectives which might give a clue to understanding their pairing mechanisms.

2. Isotope effects in multiband superconductors

Multiband superconductivity was predicted soon after the BCS theory [9–11]. The motivation for these early extensions of BCS theory was based on the observation that superconductors typically have a complex band structure with different bands crossing the Fermi level. In such a case it is possible that pairing occurs in more than one band, and pairs can be scattered between the bands. The latter assumption is essential, since independent pairing channels would give rise to different values of T_c and phase separation would set in. This implies that interband pair exchange plays a crucial role not only in ensuring a single superconducting phase and transition temperature, but also in greatly enhancing T_c [23, 24]. Even if a phonon mediated pairing glue is also assumed for a multiband BCS type superconductor, the characteristic properties of the single band model are changed in a very pronounced way [25]. The universal relation of $2\Delta/k_BT_c \approx 3.5$ (Δ is the superconducting gap) is no longer valid. The specific heat anomaly at T_c is varied, the magnetic field penetration depth deviates from BCS predictions, the isotope

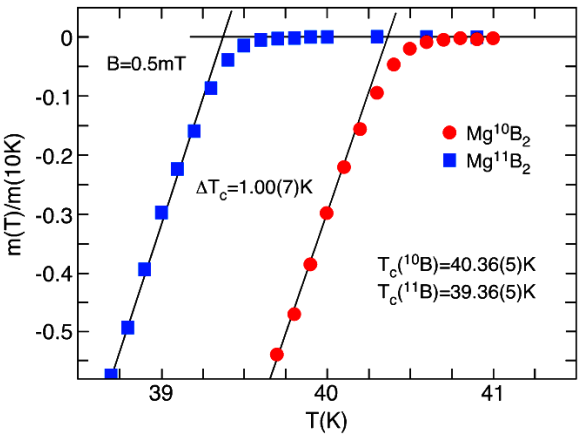

Figure 1. Field cooled ($B = 0.5$ mT) normalized magnetization m (T)/m (10 K) as a function of temperature for $Mg^{10}B_2$ and $Mg^{11}B_2$ samples. The boron isotope effect exponent is $\alpha_B = 0.29(2)$. Reproduced with permission from [30]. Copyright 2004 American Physical Society.

effect on T_c differs from the value $\alpha = 0.5$ and the pairing symmetries in the two or more bands can differ. Most of these properties were predicted early on and extensive theoretical analysis been made of multiband models [26, 27].

A systematic investigation of the isotope effect in this model has been given recently [25], where it was shown that the isotope effect is typically smaller than the BCS value and that the leading order of the gaps plays an essential role in it. In addition, it has been shown that a sign reversed isotope effect cannot occur in a multiband approach as long as anharmonicity and polaron effects can be neglected.

2.1. MgB_2

Soon after the discovery of HTS in MgB_2 [6] a finite boron-isotope ($^{10}B/^{11}B$) effect on T_c with $\alpha_B = -\partial \ln T_c/\partial \ln M_B \approx 0.3$ was reported by different groups [28–30]. An example of such an isotope effect experiment is shown in figure 1. However, only a small magnesium-isotope ($^{24}Mg/^{26}Mg$) effect with $\alpha_{Mg} = -\partial \ln T_c/\partial \ln M_{Mg} \approx 0.02(1)$ was detected [29]. It is interesting to note that the predominant contribution to the total isotope shift on T_c arises from the boron atoms in the planes where superconductivity takes place, quite analogous to layered cuprate superconductors. These boron isotope effects support a phonon mediated pairing mechanism [31–33] where a strong coupling of the B–B bond stretching E_{2g} phonon mode to the B $2p\sigma$ holes is assumed.

Since the Coulomb repulsion in MgB_2 is negligible [34], the isotope coefficient is rather small and its reduced value has been attributed to anharmonicity [35]. However, experimental and theoretical results do not support this assumption. In a recent micro-Raman study of the boron isotope effect on the E_{2g} phonon mode in the system $Mg_{1-x}Al_xB_2$ the isotope effect on this phonon mode was studied systematically as a function of x (for $0 < x < 0.57$), and a normal harmonic mass law was observed for almost all x [36]. In addition, a softening and widening of this phonon mode was seen, from which the electron–phonon coupling constant in the σ-band could be derived. These results have been used in the following to reanalyze the isotope effect using as input the data derived from the micro-Raman study [36].

Superconductivity in pure magnesium diboride is rather robust, and doping typically diminishes T_c and destroys superconductivity. Only with a single dopant, namely Al, is it possible to sustain superconductivity over rather a broad range, thus providing the possibility to study in detail the doping dependence of the superconducting energy gaps as well as of other characteristic quantities [37]. The dependence of the isotope effect on Al doping has, however, not been investigated experimentally until now. Here, we give theoretical predictions of the doping evolution of the isotope effect and show that its strong doping dependence is a consequence of the two-gap behavior with the leading gap changing its character with doping [37].

For MgB_2 it is quite generally accepted, as already pointed out above, that the B–B bond stretching E_{2g} phonon mode couples most strongly to the σ-holes and provides the pairing glue in the σ-hole channel. The second pairing channel stems from the π-electrons and the pairwise exchange between σ- and π-carriers has been shown to yield the decisive T_c enhancement mechanism [37].

The evolution of the E_{2g} phonon mode has been studied as a function of Al doping in the above mentioned paper [36] and was found to harden substantially with increasing Al content. Simultaneously, the intraband electron–phonon coupling $\lambda_{\sigma\sigma}$ decreases monotonically. Upon B isotope substitution, the expected effect of the harmonic approximation on the E_{2g} phonon mode is seen, namely that it is proportional to $1/\sqrt{M_B}$ (M_B being the boron mass) over almost the entire doping regime. Only in the vicinity of the undoped compound are small deviations observed where the phonon mode mass dependence is reduced as compared to the harmonic case. In this study the isotope effect on T_c as a function of doping has unfortunately not been measured. However, it is possible to derive this theoretically within a two-band model which has been used previously to study the Al doping dependence of the superconducting gaps, the electron–phonon couplings and T_c [37]. Since this earlier study has been proven to provide excellent agreement with later experimental data [38], we are convinced that predictions for the isotope exponent can reliably be made.

For MgB_2 and the Al doped systems the two relevant bands are the quasi-two-dimensional σ-band and the three-dimensional π-band. The Hamiltonian for this case reads [37]

$$\begin{aligned} H = &\sum_k \varepsilon_\sigma(k) c^+_{\sigma k} c_{\sigma k} + \sum_k \varepsilon_\pi(k) c^+_{\pi k} c_{\pi k} \\ &- \sum_{k,k'} V_{\sigma\sigma} c^+_{\sigma,k\uparrow} c^+_{\sigma,-k\downarrow} c_{\sigma,-k'\downarrow} c_{\sigma,k'\uparrow} \\ &- \sum_{k,k'} V_{\pi\pi} c^+_{\pi,k\uparrow} c^+_{\pi,-k\downarrow} c_{\pi,-k'\downarrow} c_{\pi,k'\uparrow} \\ &- \sum_{k,k'} V_{\sigma\pi} c^+_{\sigma,k\uparrow} c^+_{\sigma,-k\downarrow} c_{\pi,-k'\downarrow} c_{\pi,k'\uparrow} \\ &- \sum_{k,k'} V_{\pi\sigma} c^+_{\pi,k\uparrow} c^+_{\pi,-k\downarrow} c_{\sigma,-k'\downarrow} c_{\sigma,k'\uparrow} \end{aligned} \quad (1)$$

where ε_σ, ε_π are the momentum k dependent kinetic energies of σ- and π-electrons with creation and annihilation operators

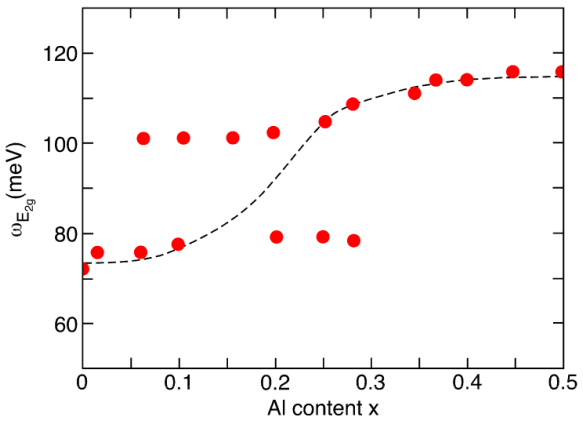

Figure 2. E_{2g} mode frequency $\omega_{E_{2g}}$ as a function of Al doping x in $Mg_{1-x}Al_xB_2$. The full circles are experimental data [36], the dashed line is the interpolated frequency used in the calculations.

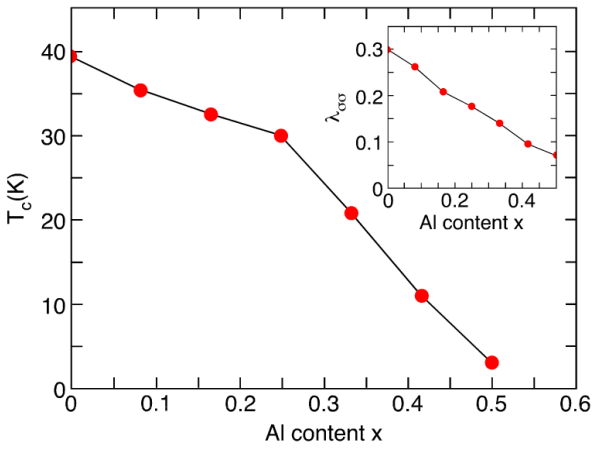

Figure 3. Superconducting transition temperature T_c as a function of Al doping x in $Mg_{1-x}Al_xB_2$. The full circles are experimental data [37], the line is the calculated x-dependence of T_c. The inset to the figure shows the calculated x-dependent intraband coupling $\lambda_{\sigma\sigma}$.

c^+, c. $V_{\sigma\sigma}, V_{\pi\pi}, V_{\sigma\pi}, V_{\pi\sigma}$ are the averaged electron–phonon interactions within the two bands and the interband interactions stemming from pairwise scattering between the $\sigma\pi$ and $\pi\sigma$ channels. The summations over k are restricted to energies within a range of $\pm\hbar\omega_{\sigma,\pi}$ which are identified with the E_{2g} mode energy in the σ-channel and an averaged phonon frequency $\omega_{\ln} = 60$ meV in the π-channel. Upon introducing the standard definitions of the effective electron–phonon couplings, $\lambda = N(E_F)V$, four coupling constants result, namely the intraband couplings $\lambda_{\sigma\sigma}, \lambda_{\pi\pi}$ and the interband couplings $\lambda_{\sigma\pi}, \lambda_{\pi\sigma}$ which are already corrected for by the corresponding intra- and interband Coulomb potentials. Equation (1) can then be re-formulated to be solved self-consistently for the coupled gaps and for the superconducting transition temperature T_c. An analytical derivation of the T_c defining equation is possible which is explicitly given by

$$k_B T_c = \sqrt{C\omega_{E_{2g}}\omega_{\ln}}\exp\left[-\frac{1}{2}\frac{\lambda_{\sigma\sigma}+\lambda_{\pi\pi}}{\tilde{\lambda}} \pm \left(\frac{1}{4}\left\{\ln\omega_{E_{2g}} + \ln\omega_{\ln} + \frac{\lambda_{\sigma\sigma}+\lambda_{\pi\pi}}{\tilde{\lambda}}\right\}^2 - \frac{1}{\tilde{\lambda}}\right)^{1/2}\right] \quad (2)$$

with $\tilde{\lambda} = \lambda_{\sigma\sigma}\lambda_{\pi\pi} - \lambda_{\sigma\pi}\lambda_{\pi\sigma}$. Obviously, the BCS isotope exponent $\alpha = 0.5$ is only observed if both phonon frequencies which enter equation (2) depend simultaneously on the same ionic mass. This is, however, not the case in Al doped MgB_2, and on the basis of equation (2) a reduced isotope exponent is expected, as also observed experimentally [28–30].

In order to derive the isotope exponent we use as input the above mentioned doping independent average frequency $\omega_{\ln}$ and the experimental E_{2g} phonon mode frequency which strongly hardens with Al doping and splits at low doping levels into a hard and a soft component [36]. This splitting is neglected in the calculation and replaced by an interpolation between the soft and the hard mode regimes (figure 2) which reflects the experimental data well.

The coupling constants have been taken from the previous approach [37], and it is worth mentioning that the doping

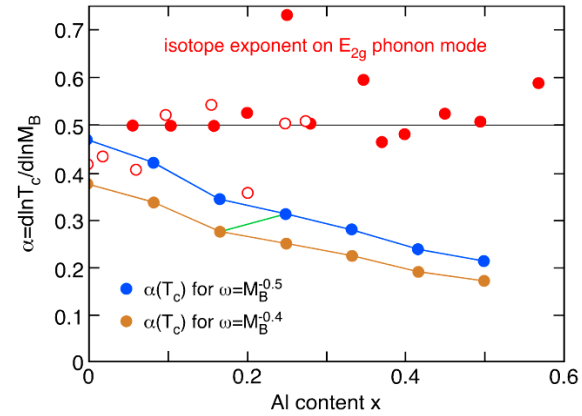

Figure 4. Isotope exponent α on T_c as a function of Al doping x in $Mg_{1-x}Al_xB_2$. The blue circles refer to α as obtained from a harmonic mass dependence of the E_{2g} mode frequency, the brown circles are the same, but assuming that the E_{2g} mode frequency is $\approx M_B^{-0.4}$. Between $x = 0.15$ and 0.25 a crossover between both behaviors is expected as indicated by the green line. The full and open red circles are the experimentally obtained isotope effects on the E_{2g} mode frequency [37]. For details refer to [37].

dependence of $\lambda_{\sigma\sigma}$ follows closely the experimentally derived one (figure 3, inset).

With the above choices T_c has been calculated as a function of Al doping x and is shown in figure 3. Note, that two regions in the x dependence of T_c are observable which exhibit distinctly different slopes, and meet at $x \approx 0.25$. This behavior has previously been noted experimentally and has been interpreted in terms of an electronic topological transition (ETT) [39]. The isotope effect on T_c is calculated by considering two cases, namely the harmonic isotope shift of the E_{2g} phonon mode with $\omega_{E_{2g}} \approx M_B^{-0.5}$ and the reduced one where $\omega_{E_{2g}} \approx M_B^{-0.4}$. The results of the calculation are shown in figure 4 together with the isotope effect on the E_{2g} phonon mode [36].

In strong contrast to BCS theory the isotope exponent depends significantly on the Al doping content x. For $x = 0$,

the value of α agrees with the experimental one if the reduced isotope effect on the E_{2g} mode is considered. With increased Al doping α systematically decreases in both cases. However, if there were the crossover of the isotope effect on the E_{2g} phonon around $x = 0.25$, an abrupt increase in α would set in around this concentration as indicated by the green line in figure 4. This could signal the occurrence of an ETT [39, 40]. The results also indicate that the coupling to the E_{2g} mode becomes less important for superconductivity which simultaneously makes the σ band less relevant, as also deduced from Raman scattering data [36].

Further isotope effects have been searched for in MgB_2, as, for example on the penetration depth [30], which would point to a polaronic pairing glue, but these were unsuccessful. It can thus be concluded from experiments and the above given theoretical analysis that MgB_2 is most likely a phonon mediated superconductor where the π-electron related band plays a less important role and the coupling to the E_{2g} phonon mode in the σ-band is the driving mechanism. It has to be kept in mind, however, that the π-band is essential in enhancing T_c, since it provides the electrons for the pairwise exchange between the two bands and the crucial increase in T_c.

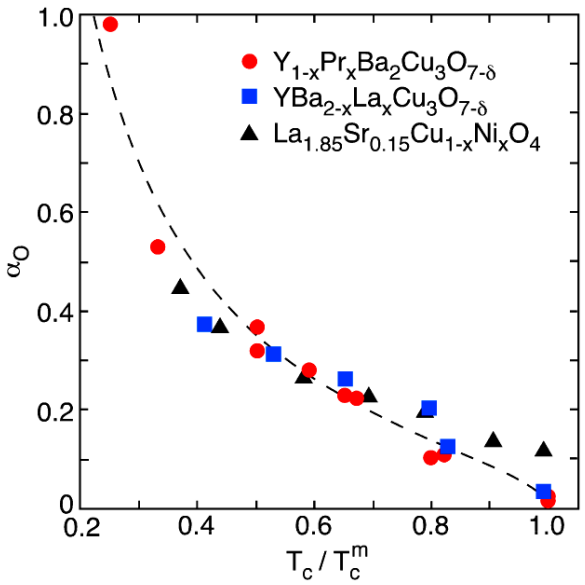

Figure 5. Oxygen isotope effect exponent α_O versus T_c/T_c^m for various families of cuprate HTSCs (T_c^m denotes the maximum T_c for a particular family). The dashed line is a guide to the eye and indicates how α_O increases with reduced T_c/T_c^m. Reproduced with permission from [46]. Copyright 2008 Elsevier.

2.2. Cuprates

Isotope effects in cuprate superconductors were investigated soon after their discovery in order to extract information on the pairing mechanism [41–43]. Conventionally this search starts with isotope effects on T_c. However, for cuprate HTSCs a huge isotope program was initiated at the University of Zurich [43], where besides of the conventional isotope effect unconventional ones were also discovered. Altogether, this comprehensive study revealed that isotope effects are present throughout the complex phase diagram of this material class [43, 44].

The starting point here is the isotope effects on T_c. Unfortunately, one of the first experiments in a large series of experiments [41–44] showed that at optimum doping the isotope effect is almost zero [45]. This finding had a biasing influence on the theory of cuprate HTSCs, since it was taken as evidence that lattice effects are not involved in the pairing mechanism. In addition, subsequent experiments, which demonstrated that the isotope effect increases substantially with underdoping and even exceeds the BCS value [41–44], have not attracted much interest and have even been frequently ignored.

The isotope effect has been investigated systematically as a function of doping [46] which is shown in a generic way in figure 5. Such a behavior is typical for cuprates and has so far not been observed in any other material class. Recently, a phenomenological explanation of its doping evolution has been given [47] based on a derivation in [48]. Importantly, site selective oxygen isotope experiments have been performed in $Y_{1-x}Pr_xBa_2Cu_3O_{7-\delta}$ with the result that the major isotope effect stems from the planar oxygen ions and an almost vanishing one from the apical and chain ions [43]. Besides this unique property, another unexpected isotope effect on the magnetic field penetration depth has been detected [43, 49–51]. This effect is completely unexpected within BCS theory and is absent in purely electronic models. The penetration depth is directly related to the superfluid carrier density and its inverse effective mass. This effect was interpreted early on in terms of polaron formation [52, 53] where both the carrier density and the effective mass have been discussed as its origin. A more consistent explanation has been offered in a variety of works where polaronic band narrowing was shown to be responsible for almost all the observed isotope effects [54–56]. Note that no appreciable boron ($^{10}B/^{11}B$) isotope effect on the magnetic penetration depth has been detected in MgB_2 [30], indicating that the pairing in this system is more conventional phonon mediated than polaronic in nature.

Another unexpected isotope effect has been seen on the pseudogap temperature T^* [57–59], which—opposite to the isotope effect on T_c—shifts to higher temperatures with the heavier isotope. Within the above mentioned model [54–56] it has been demonstrated that polaron formation has the effect of local mode phonon softening which, in turn, yields the reversed isotope effect on T^* [46, 47, 54–56].

Finally, isotope effects on the phase diagram of cuprates [44] have to be mentioned. A summary of these is shown in figure 6 where all phases of the phase diagram are displayed. In the undoped antiferromagnetic phase the isotope effect on T_N increases from almost zero to large negative values, and continues to remain negative upon entering the spin glass phase. In the coexistence regime of the spin glass phase and superconductivity a two-component isotope effect is seen, which seems to be related to phase separation, namely a negative one on the spin glass freezing temperature T_{SG} and a conventional but unusually large one on T_c. The latter effect diminishes with increasing doping to nearly vanish at optimum T_c.

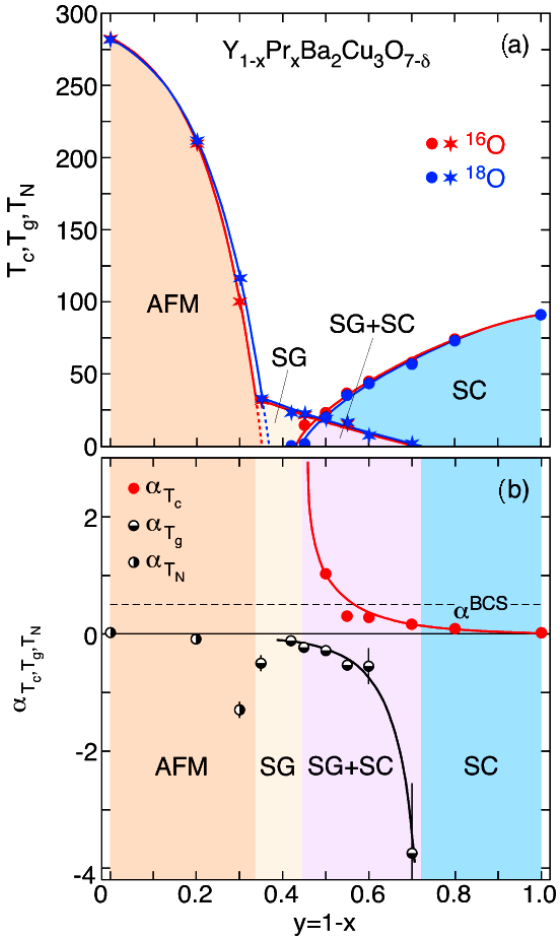

Figure 6. (a) Dependence of the superconducting transition temperature T_c, the spin glass transition temperature T_g, and the Néel temperature T_N for $^{16}O/^{18}O$ substituted $Y_{1-x}Pr_xBa_2Cu_3O_{7-\delta}$ on the Pr content $y = 1 - x$. The solid lines are guides to the eye. The areas denoted by AFM, SG, and SC represent the antiferromagnetic, the spin glass, and the superconducting regions, respectively. In the region SG + SC spin glass magnetism and superconductivity coexist. (b) Dependence of the corresponding oxygen-isotope-effect exponents $\alpha(T_c)$, $\alpha(T_g)$, and $\alpha(T_N)$ as a function of $y = 1 - x$. The dashed line corresponds to the BCS value $\alpha(T_c - \text{BCS}) = 0.5$. The solid lines are guides to the eye. Reproduced with permission from [44]. Copyright 2008 American Physical Society.

The analysis of the above mentioned isotope effects in terms of a polaronic model has provided convincing agreement with experiment [46, 57–60]. However, and opposite to MgB_2, analytic expressions for these isotope effects are absent and only numerical results can be given. The main origin of this situation relates to the fact that polaron formation induces a band narrowing, i.e. a reduction of the electronic kinetic energy. Two limiting cases exist here, which are rather irrelevant to the interesting physical regime [2]. For strong polaronic coupling the reduction in kinetic energy is so large that localization sets in and superconductivity is lost. When the coupling is negligibly small, itinerant electronic behavior takes place and only BCS type conventional superconductivity will be observed. The interesting regime is the one in between both limits, where both energy scales, the polaron binding energy and the band energy, are comparable [2]. This is what we are convinced happens in cuprates. Another important property of these ideas is—and this is in strong contrast to related work [52, 53, 61]—that the polarons do not form homogeneously on the lattice but only around the dopant, thereby creating intrinsic dynamic heterogeneity which orders at T^* into striped like dynamical patterns.

2.3. Fe based superconductors

After the 2008 discovery of superconductivity in FeAs based layered systems [12], a certain revival in superconductivity research occurred, especially when it was shown that T_c can be as large as 56 K [13], i.e. increasing the T_c of MgB_2 by 40%. The following stagnation in T_c has, however, destroyed the hope of reaching liquid nitrogen temperatures and breaking the cuprates record T_cs. The pairing mechanism in pnictides and related Fe derived systems was addressed immediately after their discovery. It has been argued from theoretical considerations [62] based on inelastic neutron scattering experiments [63, 64] that the electron–phonon mechanism is too weak [62] to explain the high T_cs. Again purely electronic models have been stressed for the pairing mechanism [65, 66]. In addition, the antiferromagnetic properties of the undoped parent compounds have revealed a certain analogy with cuprate HTSCs. On the other hand, it was rapidly proven that pnictides are not in the strongly correlated limit but are more conventionally Fermi liquid like [67], which brings into question whether antiferromagnetic pairing fluctuations are the pairing glue. The interesting correlations between structural properties and the superconducting phase have been emphasized in [68, 69].

Quite unlike in the cuprates, the investigation of an isotope effect on T_c in Fe based superconductors is very demanding, since, like the $^{16}O/^{18}O$ exchange in cuprates for example, an *in situ* exchange of Fe or other constituents such as As by their isotopes is impossible. This requires that statistics over many samples with the same preparation techniques and growth conditions have to be performed in order to unambiguously arrive at conclusions about a possible isotope effect [22]. An additional complication arises from the fact that Fe based superconductors like MgB_2 are multi-gap superconductors, where isotope effects can result from different pairing mechanisms in the different channels.

Almost simultaneously two groups have performed the Fe isotope exchange in nominally identical FeAs based compounds [20, 21]. Rather disappointingly, both groups arrived at controversial results, namely a conventional isotope exponent of $\alpha_{Fe} \approx 0.35$ [20] and a sign reversed one of $\alpha_{Fe} \approx -0.2$ [21]. Shortly afterwards the same group who reported the sign reversed isotope exponent published another isotope study, but with a negligibly small value of $\alpha_{Fe} \approx -0.02$ [70]. As such a rather unusual situation emerged which could be partially clarified by an independent third study [22], where statistics were invoked and a rather large isotope effect of $\alpha_{Fe} \approx 0.8$ was found (figure 7). Importantly, in this last experiment it was observed that the isotope exchange was accompanied by small structural modifications [22], which,

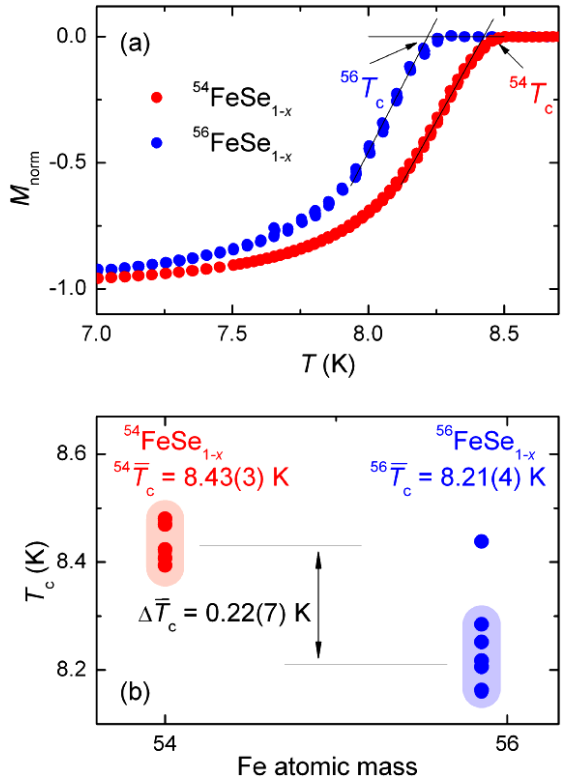

Figure 7. (a) Zero-field cooled normalized magnetization curve of one pair of ^{54}FeSe$_{1-x}$and ^{56}FeSe$_{1-x}$ samples. (b) The superconducting transition temperature T_c as a function of the Fe atomic mass for a series of ^{54}FeSe$_{1-x}$ and ^{56}FeSe$_{1-x}$ samples studied in [22]. The T_cs fall into two regions marked by the colored stripes, corresponding to an ^{54}Fe/^{56}Fe isotope exponent of $\alpha_{Fe} = 0.85(15)$. Adapted from [22].

in view of the sensitivity of T_c to tiny structural alterations, could substantially modify the isotope effect. A very careful analysis of these structural changes has been carried through subsequently [71], with the result that if these are taken into account the isotope effect reduces to values similar to those observed in the first study, namely $\alpha_{Fe} \approx 0.35$–0.40 (figure 8).

3. Multiband signatures

3.1. MgB_2

Soon after the discovery of HTS in MgB_2 tunneling data provided convincing evidence that MgB_2 is a multiband superconductor [8]. Two types of carriers contribute to the superconducting condensate, namely, B related σ-electrons and Mg related π-electrons. The corresponding superconducting gaps are 7.9 meV and 2.1 meV, respectively. The fact that both gaps close simultaneously at a single transition temperature is due to interband interactions where σ-band pairs are scattered into π-pairs and vice versa [8]. Without this interband interaction only the σ-electrons would exhibit superconductivity with a strongly reduced T_c of 18 K [37]. This fact demonstrates that the interband interaction is the driving term to enhance T_c enormously, independent of the fact that the π-band alone would not exhibit superconductivity at all. In spite of this latter

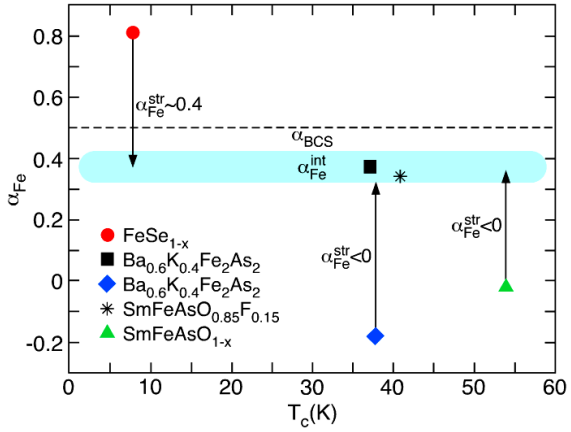

Figure 8. Fe isotope effect exponent α_{Fe} as a function of T_c for the iron based superconductors discussed in this work: FeSe$_{1-x}$ [22], Ba$_{0.6}$K$_{0.4}$Fe$_2$As$_2$ and SmFeAsO$_{0.85}$F$_{0.15}$ [20], Ba$_{0.6}$K$_{0.4}$Fe$_2$As$_2$ [21], and SmFeAsO$_{1-x}$ [70]. Arrows indicate the correction caused by structural effects. Note that $\alpha^{int}_{Fe} \approx 0.35$–$0.40$ for all samples ($\alpha_{BCS} = 0.5$ denotes the weak-coupling BCS value). See text for details. Adapted from [71].

consideration the role of the π-electrons gains a new importance since they contribute via pairwise exchange to the high T_cs. An interesting crossover in the leading gap takes place with Al doping [37]. Even though any doping of MgB_2 always leads to a rapid suppression of superconductivity, Al doping can be carried through up to 43% Al content with superconductivity persisting [37]. As has already been shown above, the electron–phonon interaction in the leading gap decreases with increasing Al doping, evidenced by a hardening of the E_{2g} B–B bond stretching mode [36]. In the π-channel, on the other hand, the phonon mode remains almost unaffected by doping [36], thus leaving the related electron–phonon coupling nearly constant. By taking these facts into account, the evolution of the two gaps with Al doping can be calculated and is shown in figure 9 (left). While the intraband interactions follow the above described doping dependence, i.e. decreasing rapidly in the σ-channel and staying almost constant in the π-channel, the interband interaction has a small doping dependence with a rounded maximum around $x = 0.75$ in $Al_{1-x}Mg_xB_2$ (figure 9, right). At this doping level also the crossover in the leading gap takes place, the π-gap becoming dominant over the σ-gap.

An interesting correlation of the gap to T_c ratios is a consequence of the two-band model. In Al doped MgB_2 this relation is nicely followed at all doping levels, namely, that the average gap $\bar{\Delta} = \sqrt{\Delta_\sigma^2 + \Delta_\pi^2}$ to T_c ratio remains in the BCS limit of $2\bar{\Delta}/k_B T_c \approx 3.52$. This is shown in figure 10 where the individual gap to T_c ratios are plotted as a function of x. It is important to emphasize here that this observation is directly related to the fact that both gaps have s-wave symmetry. For other order parameter symmetry combinations also a fixed relation between the average gap to T_c ratio are obeyed, but with values deviating distinctively from the BCS value.

3.2. Cuprates

Unlike MgB_2 and Fe based superconductors there is no general agreement on the existence of multiband

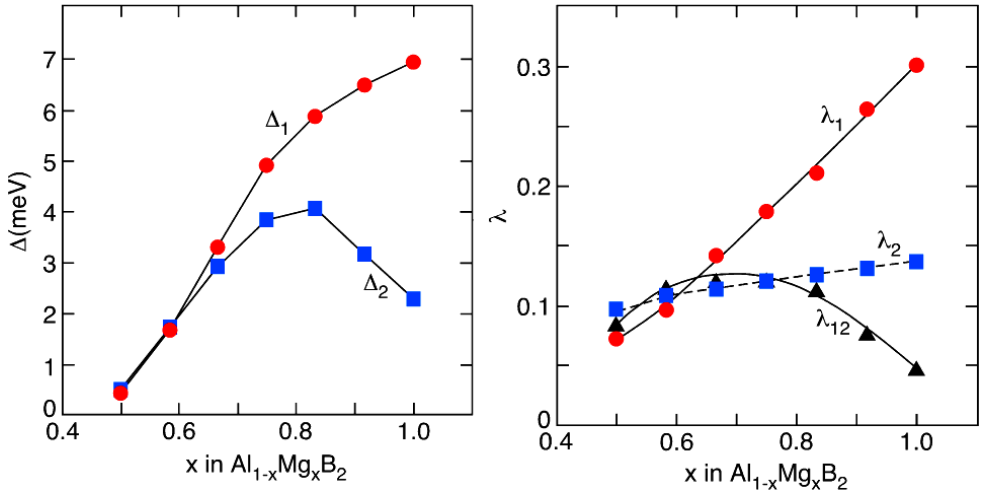

Figure 9. (left) Theoretically derived energy gaps Δ_1 related to the σ-band and Δ_2 related to the π-band as a function of Al doping x. (right) The screened effective couplings $\lambda_1(x)$ and $\lambda_2(x)$ for the σ- and π-electrons, respectively. The interband coupling $\lambda_{12}(x)$ has been calculated in such a way as to reproduce the experimental values of T_c for each x.

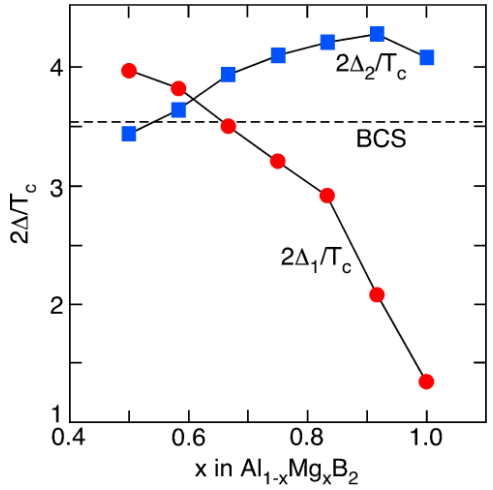

Figure 10. The energy gaps to T_c ratios (Δ_1 related to the σ-band and Δ_2 related to the π-band) at $T = 0$ K as a function of Al doping$x$.

superconductivity in cuprate HTSCs. Theoretically, electronic models assume that the superconducting gap is of purely d-wave symmetry as required by symmetry considerations on a 'square' lattice and the fact that the Hubbard U becomes attractive at the antiferromagnetic wavevector, i.e. a sign reversal in the gap function has to be present. In addition, the homogeneity of the ground state, as postulated in these models, does not admit for admixtures of other order parameter symmetries. These ideas were supported early on by tricrystal experiments [72], which were later repeated and corrected by admitting that a purely d-wave order parameter does not fit with the experiment [73]. On the other hand, soon after the discovery of cuprates Raman scattering data showed that a single order parameter approach is inconsistent with the experiment and that s+d wave superconductivity, i.e. two-gap superconductivity, can explain the data [74]. In line with these experiments tunneling along the c-axis did only find s-wave superconductivity without any d-wave contribution [75]. Ten years after the discovery of HTS [76, 77] the proposal was made that cuprates have s + d wave symmetry simply due to the fact that many experiments including nuclear magnetic resonance and nuclear quadrupole resonance are inconsistent with a single d-wave order parameter. These ideas were subsequently followed by the University of Zurich group. Since the temperature dependence of the penetration depth $\lambda(T)$ is particularly sensitive to the gap symmetry, bulk testing experiments have been performed to extract $\lambda(T)$ along different crystallographic directions. Various families of cuprate HTSCs have been investigated and a rather unique picture appeared from these μSR data [46, 78–82]. For all samples the in-plane $\lambda_{ab}(T)$ shows an inflection point at low temperatures, also when it was possible to measure a and b directions separately. Along the c-direction the temperature dependence is qualitatively different from the in-plane data, since there the inflection point is absent and the temperature dependence of $\lambda_c(T)$ follows the BCS predictions for an isotropic s-wave gap (figure 11).

By analyzing the data within a two-component model with coupled s + d-wave order parameters [46, 54–56], quantitative agreement between experiment and theory could be achieved. It is clear from the analysis that the s-wave gap contributes much less to the superfluid density compared to the d-wave gap, but that its contribution is essential in order to understand the data. It has been argued that the orthorhombic distortion, present in almost all cuprates, gives rise to the mixed order parameter behavior [73]. This, however, cannot be the case since this distortion is small and cannot account for at least 35% of the s-wave contribution. In view of the fact that various cuprate families have consistently shown the same behavior of $\lambda(T)$, we are convinced that it is generic to cuprate HTSCs and reflects the intrinsic inhomogeneity of these materials. Typical s- and d-wave gaps and their temperature dependence are shown in figure 12.

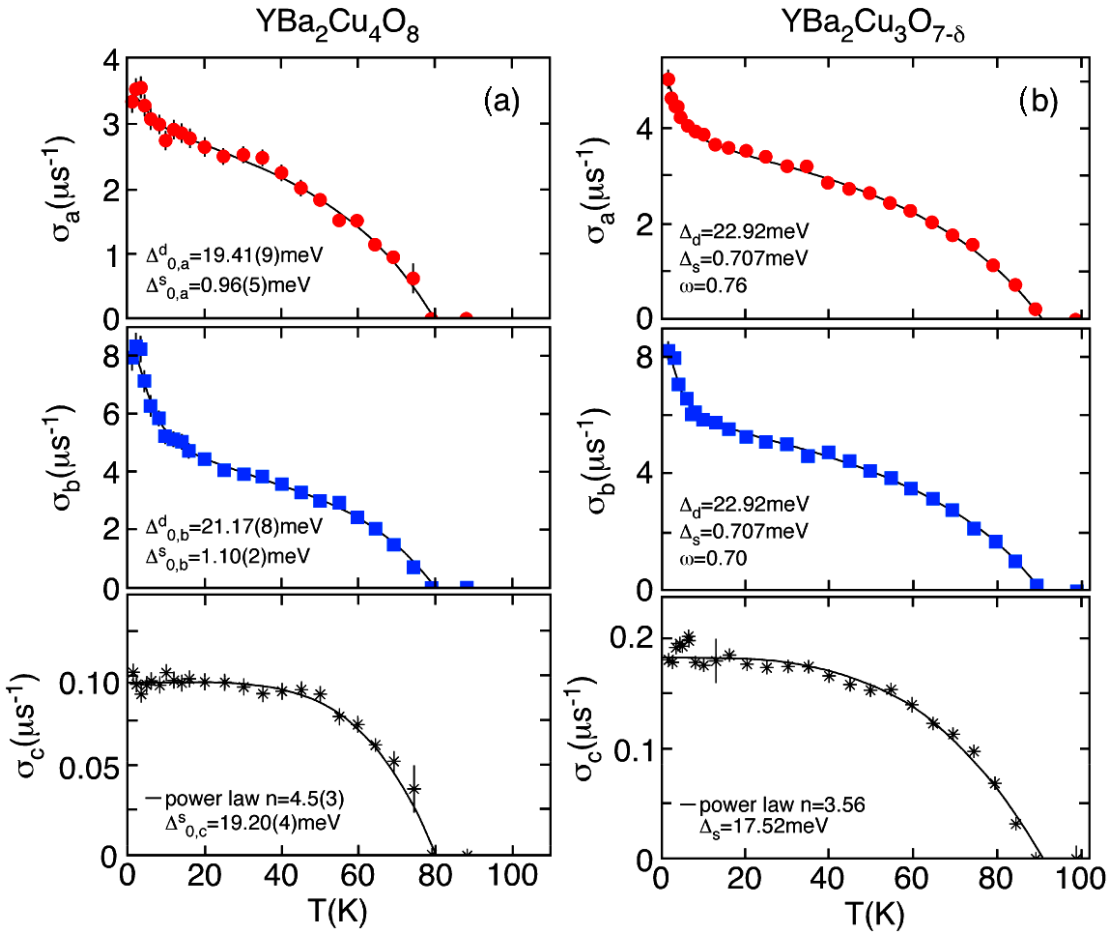

Figure 11. (a) Temperature dependence of the μSR relaxation rate $\sigma_a \propto \lambda_a^{-2}$, $\sigma_b \propto \lambda_b^{2}$, and $\sigma_c \propto \lambda_c^{-2}$ of single crystal $YBa_2Cu_4O_8$ measured along the three principal axes a, b, and c. (b) Temperature dependence of the μSR relaxation rate $\sigma_a \propto \lambda_a^{-2}$, $\sigma_b \propto \lambda_b^{-2}$, and $\sigma_c \propto \lambda_c^{-2}$ of single crystal $YBa_2Cu_3O_{7-\delta}$ measured along the three principal axes a, b, and c. The solid lines represent model calculations explained in the text. Adapted from [79, 80].

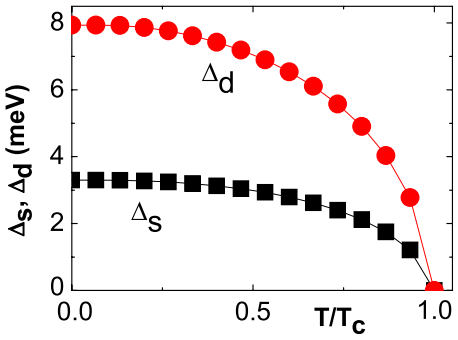

Figure 12. The calculated energy gaps Δ_s and Δ_d as a function of T/T_c for optimally doped $La_{2-x}Sr_xCuO_4$.

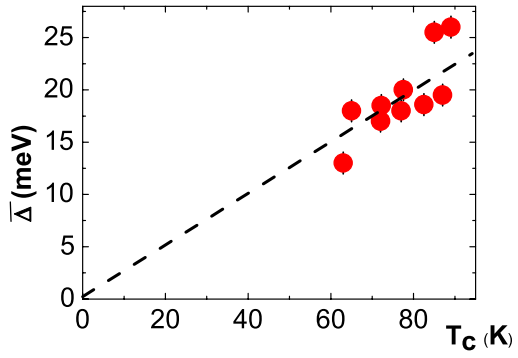

Figure 13. The calculated average energy gap $\bar{\Delta} = \sqrt{\Delta_s^2 + \Delta_d^2}$ as a function of T_c (dashed line) compared to experimental data from [85] (full circles).

They seem to follow individually the BCS relations, however, and unlike MgB_2, their average does not obey the BCS value in relation to T_c but is largely enhanced over it (figure 13). This average has been calculated for a variety of systems and is seen to lie on a single line [83, 84]. The enhancement of $2\bar{\Delta}/kT_c$ can be attributed to the s + d wave combination of the order parameter and is in good agreement with experimental data.

3.3. Fe based superconductors

The unusually high superconducting transition temperatures of the newly discovered Fe–As based superconductors [12, 13] and their proximity to a magnetic ground state have been taken as evidence that the origin of superconductivity

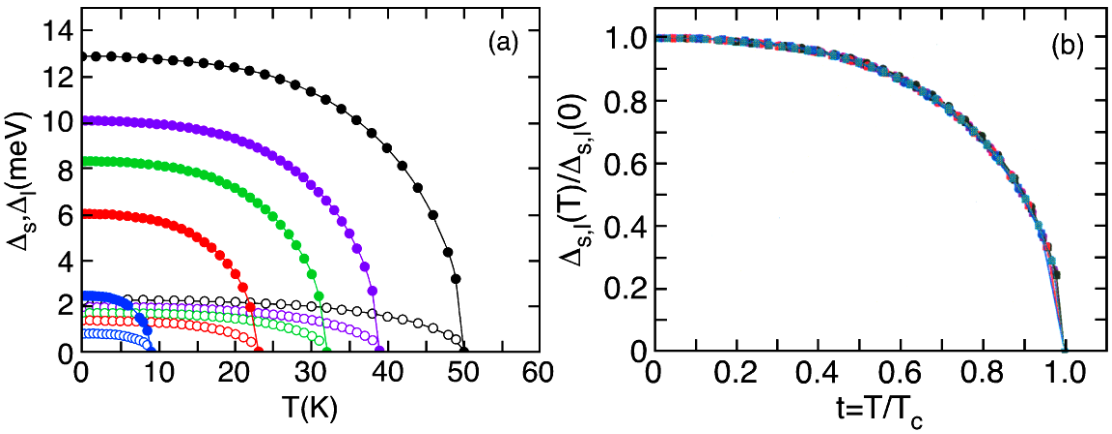

Figure 14. (a) Temperature dependence of the small (Δ_s open symbols) and the large (Δ_l full symbols) gap for various values of T_c. (b) The normalized gap values are displayed in (a) as functions of $t = T/T_c$. Reproduced with permission from [104]. Copyright 2011 Springer Science and Business Media.

might be unconventional and related to magnetic fluctuations. Also, the observation of only small phonon responses at the onset of superconductivity [63, 64] together with numerical results [62] have prompted some groups to advocate an exotic non-phononic pairing mechanism [65, 66]. However, unlike cuprates, in most pnictides a sharp line separates the magnetic phase from the superconducting one, which suggests that these phenomena are not related to each other. Another important finding is the observation of multiple gaps either detected directly through tunneling experiments [86–89] and angle resolved photoemission studies (ARPES) [90–92] or indirectly through the temperature dependence of the superfluid density [93–98], the heat transport [99, 92], and the lower critical field [97] where nodeless gaps with s-wave symmetry have been observed.

The Fermi surface of Fe–As based superconductors is complex with diverse electron and hole type sheets which might give rise to multiple superconducting gaps [100, 101]. While in most experiments which measure the superconducting gaps only two gaps are seen, there are a few exceptions reporting more than two gaps [90–92] (where, however, two gaps exhibit almost the same value). Since two flat bands have been identified along the Γ–Z and A–M high symmetry directions [102], the complexity can be reduced to a two-gap problem, both with s-wave symmetry, since this seems to be indicated experimentally. It has to be noted that some data are compatible with line nodes in the gap [103], but the features observed in [40] can also be a consequence of the coexistence of coupled s-wave gaps. The coupled gap relations are derived from an effective two-band extended BCS Hamiltonian with interband interactions, as was also introduced above for the case of MgB_2. The bands are Fe d–As p hybridized. This hybridization is crucial since the magnetic properties of the parent compounds are strongly dependent on it [100]. In addition, it is assumed that a band with large density of states leading to a dominant gap is present which induces superconductivity via interband interactions in the second band with a small density of states. Such a scenario corresponds to almost localized states coupled via a highly dispersive band to another small density flat band. Since the formal derivation of the coupled gap equations has already been given in section 2.1, we note here only that in the Fe based superconductors an analogous analysis can be performed, from which some unique properties emerge regarding the temperature dependence of the coupled gaps and their dependence on T_c. Rather in contrast to MgB_2 and its Al doped compounds is the fact that in Fe based HTSCs one gap is always distinctively smaller than the other one and a gap crossing, as seen in Al doped MgB_2 seems to be absent. Within such a scenario superconductivity is induced via interband coupling in the smaller gap. The numerically derived coupled gaps are shown as a function of T_c for this modeling in figure 14(a). In figure 14(b) the normalized gaps $\bar{\Delta}_i(T)/\bar{\Delta}_i(0)$ versus normalized temperature $t = T/T_c$ are shown. All values for the gaps, the small and large ones, fall on a single line. This scaling relation is not observed in systems where the coupled gaps have different order parameter symmetries [76]. It is thus possible to draw conclusions about the symmetry of the order parameters from the temperature dependence of the normalized gap values. Note that, in the case of coupled d-wave order parameters, a linear in T term should appear at low temperatures which is absent for s-wave gaps [37].

Besides the universal T-dependence of the normalized energy gaps, the gap to T_c ratios exhibit interesting properties. For instance, for Al doped MgB_2 this ratio is substantially reduced for the smaller gap and enhanced for the larger one [37]. The average of both gaps is, however, in the BCS limit. This relation is again not fulfilled in a multiband superconductor with different pairing symmetries: Typically a d-wave order parameter leads to an appreciable enhancement over the BCS relation [105]. In figure 15(a) the gap to T_c ratios and their average are shown for the above introduced model. A significant resemblance to Al doped MgB_2 exists, where the average ratio is again within the BCS value.

However, a small but systematic dependence on T_c is present: the ratio is slightly enhanced for small values of T_c, decreasing continuously to the BCS value with increasing T_c. In figure 15(b) the individual gap values are displayed as a function of T_c together with experimentally determined gap

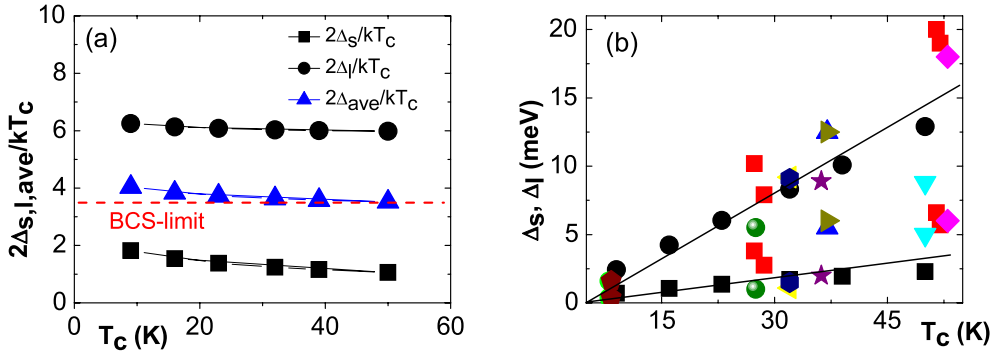

Figure 15. (a) The individual and average gap to T_c ratios as a function of T_c. (b) Energy gap values for the corresponding values of T_c (black symbols and lines). The colored symbols refer to experimental data: red squares [86], green diamonds [99], blue up triangles [90], magenta diamonds [88], cyan down triangles [87], yellow left triangles [92], dark yellow right triangles [91], navy hexagons [95], purple stars [97], wine up squares [98], olive balls [89]. Reproduced with permission from [104]. Copyright 2011 Springer Science and Business Media.

Table 1. Summary of the relevant quantities related to the two-band model discussed in the text. The first column shows the values of T_c, the second, third, and fourth columns display the density of states times the interaction constants in the small, large intraband and interband terms. The absolute gap values for the small and large gaps are given in the next two columns. The last three columns refer to $2\Delta/kT_c$ ratios for small, large, and average gaps. After [105].

T_c (K)	$N_lV_l(0)$	$N_sV_s(0)$	$N_{sl}V_{sl}(0)$	$\Delta_l(0)$ (meV)	$\Delta_s(0)$ (meV)	$2\Delta_s/kT_c$	$2\Delta_l/kT_c$	$2\bar{\Delta}/kT_c$
9	0.208	0.018	0.06	2.42	0.71	1.82	6.25	4.04
16	0.242	0.018	0.06	4.23	1.06	1.54	6.13	3.84
23	0.268	0.018	0.06	6.03	1.37	1.38	6.08	3.73
32	0.297	0.018	0.06	8.32	1.71	1.24	6.03	3.64
39	0.317	0.018	0.06	10.09	1.95	1.16	6.00	3.58
50	0.346	0.018	0.06	12.9	2.29	1.06	5.98	3.52

values. The comparison between both is rather convincing in spite of the huge scatter in the experimental data. It is important to emphasize again that only the intraband interaction in the band, where the dominant gap opens, is varied with T_c (see table 1), whereas we hold the interaction in the band related to the smaller gap constant. In addition, the interband interaction is also held fixed for all investigated systems. In spite of these simplifications, obviously the smaller gap adopts a significant dependence on T_c which implies that the coupling between the gaps influences the smaller one to increase systematically with the larger one. The gap coupling together with the intraband coupling of the larger gap thus induces a substantial increase of the smaller gap with increasing T_c. The dependence of both gaps on T_c deviates from linearity, which is most pronounced for small values of T_c.

4. Conclusion

In the preceding paragraphs we have summarized isotope and multiband effects in the three layered HTSC classes: MgB_2, cuprates, and Fe based systems. In all three of them isotope effects on T_c have been observed, but in very distinct ways. While the rather small boron isotope effect on T_c in MgB_2 can be fully explained as stemming from a strong coupling of the σ-electrons to the B–B E_{2g} vibration, and diminished as compared to the BCS value due to the presence of a second superconducting channel, the one observed in cuprates does not find such a straightforward explanation. Here the strong doping dependence of the isotope effect on T_c and its large values at the border to the antiferromagnetic state require an interaction different from phonon mediated pairing. This is offered here in terms of polaron formation around the dopant. Opposite to MgB_2, and still unknown for Fe based superconductors, an isotope effect on the penetration depth has been reported which can very consistently be explained by polaronic effects. In addition, the complete phase diagram, ranging from insulating antiferromagnetic via spin glass and coexistence phases to superconductivity alone, exhibits isotope effects. For the Fe based HTSCs the situation is unclear and requires many more experimental studies. An isotope effect on T_c has been reported, but with controversial results. These could converge if the tiny structural changes accompanying the isotopic substitution are thoroughly taken into account. An isotope effect on the penetration depth similar to a doping dependent one on T_c has not yet been measured.

Multiband superconductivity is not questioned for MgB_2. In spite of the rather small gap in the π-channel, the two superconducting gaps are important for the T_c enhancement due to the interband interactions. In addition, a crossing of the leading gap sets in with Al doping which has not yet been observed in other systems.

In cuprates s + d wave superconductivity was postulated from the very beginning, but has frequently been ignored since inconsistencies with theoretical models appeared. Rather recently performed measurements of the penetration depth, have, however, proven their existence and shown that the

s + d wave character is dominant in the CuO planes whereas along the *c*-direction an almost 100% s-wave order parameter is realized. This finding has the important consequence that cuprates are intrinsically inhomogeneous, which can be related to local polaron formation.

In Fe based superconductors the majority of experimental data support multiband superconductivity. There is, however, no consensus about the symmetry of the coupled order parameters. While predominantly two s-waves gaps are reported, some experiments are in favor of gaps with nodes.

For all three cases discussed here, it can be inferred that the high superconducting transition temperatures are a consequence of gap coupling and interband interactions which easily raise T_c to the observed values.

This summary of isotope and multiband effects in the layered HTSCs does not provide an answer to the pairing mechanism in these compounds. It does, however, show that purely electronic approaches are at least incomplete and inhomogeneity and structural effects have peculiar influences on superconductivity.

Acknowledgments

It is our pleasure to acknowledge many supporting and clarifying discussions with K A Müller, A Simon, A Shengelaya, R Khasanov, S Weyeneth, M Bendele, and S Strässle.

References

[1] Bednorz J G and Müller K A 1986 *Z. Phys.: Condens. Matter* **64** 189
[2] Höck K-H, Nickisch H and Thomas H 1983 *Helv. Phys. Acta* **56** 237
[3] Bednorz J G and Müller K A 1988 *Rev. Mod. Phys.* **60** 585
[4] Müller K A 1966 *Magnetic Resonance and Relaxation* ed R Blinc (Amsterdam: North Holland) pp 192–208
[5] Schilling A, Cantoni M, Guo J D and Ott H R 1993 *Nature* **363** 56
[6] Jun N, Norimasa N, Takahiro M, Yuji Z and Jun A 2001 *Nature* **410** 63–4
[7] Choi H J, Roundy D, Sun H, Cohen M L and Loie S G 2002 *Nature* **418** 758
An J and Pickett W E 2001 *Phys. Rev. Lett.* **86** 4366
De la Peña-Seaman O, de Coss R, Heid R and Bohnen K-P 2010 *Phys. Rev.* B **82** 224508
[8] Special issue on MgB_2 2003 *Physica* **385C** see articles in sections 7 and 8
[9] Moskalenko V 1959 *Fiz. Metal. Metalloved.* **8** 503
[10] Suhl H, Matthias B T and Walker L 1959 *Phys. Rev. Lett.* **3** 552
[11] Kondo J 1963 *J. Progr. Theor. Phys.* **29** 1
[12] Kamihara Y, Watanabe T, Hirano M and Hosono H 2008 *J. Am. Chem. Soc.* **130** 3296
[13] Chen G F, Li Z, Wu D, Li G, Hu W Z, Dong J, Zheng P, Luo J L and Wang N L 2008 *Phys. Rev. Lett.* **100** 247002
Zhu X Y, Yang H, Fang L, Mu G and Wen H-H 2008 *Supercond. Sci. Technol.* **21** 105001
Chen X H, Wu T, Wu G, Liu R H, Chen H and Fang D F 2008 *Nature* **453** 761
Ren Z A *et al* 2008 *Chin. Phys. Lett.* **25** 2215
Johrendt D and Pöttgen R 2008 *Angew. Chem. Int. Edn* **47** 4782
Tegel M, Bichler D and Johrendt D 2008 *Solid State Sci.* **10** 193
[14] Park J T *et al* 2009 *Phys. Rev. Lett.* **102** 117006
[15] Aczel A *et al* 2008 *Phys. Rev.* B **78** 214503
Goko T *et al* 2009 *Phys. Rev.* B **80** 024508
[16] Sanna S, De Renzi R, Lamura G, Ferdeghini C, Palenzona A, Putti M, Tropeano M and Shiroka T 2009 *Phys. Rev.* B **80** 052503
Drew A J *et al* 2009 *Nature Mater.* **8** 310
[17] Khasanov R *et al* 2009 *Phys. Rev.* B **80** 140511
[18] Luetkens H *et al* 2009 *Nature Mater.* **8** 305
[19] Johnston D C 2010 *Adv. Phys.* **59** 803
[20] Liu R H *et al* 2009 *Nature* **459** 64
[21] Shirage P M, Kihou K, Miyazawa K, Lee C-H, Kito H, Eisaki H, Yanagisawa T, Tanaka Y and Iyo A 2009 *Phys. Rev. Lett.* **103** 257003
[22] Khasanov R, Bendele M, Conder K, Keller H, Pomjakushina E and Pomjakushin V 2010 *New J. Phys.* **12** 073024
[23] Bussmann-Holder A, Micnas R and Bishop A R 2003 *Eur. Phys. J.* B **37** 345
[24] Bussmann-Holder A, Bishop A R, Büttner H, Egami T, Micnas R and Müller K A 2001 *J. Phys.: Condens. Matter* **13** L545
Bussmann-Holder A, Müller K A, Micnas R, Büttner H, Simon A, Bishop A R and Egami T 2001 *J. Phys.: Condens. Matter* **13** L169
[25] Bussmann-Holder A, Keller H, Khasanov R, Simon A, Bianconi A and Bishop A R 2011 *New J. Phys.* **13** 093009
[26] Geilikman B, Zaitsev R and Kresin V Z 1967 *Sov. Phys.—Solid State* **9** 524
[27] Kresin V and Wolf S 1990 *Physica* C **169** 476
Kresin V, Wolf S and Deutscher G 1992 *Physica* **191** 9
Kresin V and Wolf S 1990 *Phys. Rev.* B **41** 4278
Kresin V and Wolf S 1992 *Phys. Rev.* B **46** 6458
[28] Bud'ko S L, Lapertot G, Petrovic C, Cunningham C E, Anderson N and Canfield P C 2001 *Phys. Rev. Lett.* **86** 1877
[29] Hinks D G, Claus H and Jorgensen J D 2001 *Nature* **411** 457
Hinks D G and Jorgensen J D 2003 *Physica* C **385** 98
[30] Di Castro D *et al* 2004 *Phys. Rev.* B **70** 014519
[31] Kong Y, Dolgov O V, Jepsen O and Andersen O K 2001 *Phys. Rev.* B **64** 020501(R)
[32] Boeri L, Kortus J and Andersen O K 2004 *Phys. Rev. Lett.* **93** 237002
[33] Mazin I I and Antropov V P 2003 *Physica* C **385** 49
[34] Golubov A A, Kortus J, Dolgov O V, Jepsen O, Kong Y, Andersen O K, Gibson B J, Ahn K and Kremer R K 2002 *J. Phys.: Condens. Matter* **14** 1353
[35] Yildirim T *et al* 2001 *Phys. Rev. Lett.* **87** 037001
[36] Simonelli L, Palmisano V, Fratini M, Filippi M, Parisiadis P, Lampakis D, Liarokapis E and Bianconi A 2009 *Phys. Rev.* B **80** 014520
[37] Bussmann-Holder A and Bianconi A 2003 *Phys. Rev.* B **67** 132509
[38] Cooley L D, Zambano A J, Moodenbaugh A R, Klie R F, Zheng J-C and Zhu Y 2005 *Phys. Rev. Lett.* **95** 267002
[39] Lifshitz I M 1960 *Sov. Phys.—JETP* **11** 1130
Bianconi A 2005 *J. Supercond.* **18** 25 and references therein
[40] Caivano R *et al* 2009 *Supercond. Sci. Technol.* **22** 014004
[41] Franck J P 1994 *Physical Properties of High Temperature Superconductors IV* ed D M Ginsberg (Singapore: World Scientifc) p 94
[42] Crawford M K, Kunchur M N, Farneth W E, McCarron E M III and Poon S J 1990 *Phys. Rev.* B **41** 282
[43] Keller H 2005 *Superconductivity in Complex Systems* (*Springer Series Structure and Bonding* vol 114) ed K A Müller and A Bussmann-Holder (Heidelberg: Springer) p 43

[44] Khasanov R, Shengelaya A, Di Castro D, Morenzoni M, Maisuradze A, Savic I M, Conder K, Pomjakushina E, Bussmann-Holder A and Keller H 2008 *Phys. Rev. Lett.* **101** 077001

[45] Batlogg B *et al* 1987 *Phys. Rev. Lett.* **58** 2333

[46] Keller H, Bussmann-Holder A and Müller K A 2008 *Mater. Today* **11** 38

[47] Weyeneth S and Müller K A 2011 *J. Supercond. Nov. Magn.* **42** 1235

[48] Kresin V Z and Wolf S A 1994 *Phys. Rev.* B **49** 3652

[49] Zhao G M, Conder K, Keller H and Müller K A 1998 *J. Phys.: Condens. Matter* **10** 9055

[50] Müller K A 2000 *Physica* C **341–348** 11

[51] Zhao G M, Keller H and Conder K 2001 *J. Phys.: Condens. Matter* **13** R569

[52] Bill A, Kresin V Z and Wolf S 1998 *Phys. Rev.* B **57** 1257

[53] Alexandrov A S 1992 *Phys. Rev.* B **46** 14932

[54] Bussmann-Holder A, Keller H and Müller K A 2005 *Superconductivity in Complex Systems* (*Springer Series Structure and Bonding* vol 114) ed K A Müller and A Bussmann-Holder (Heidelberg: Springer) p 367

[55] Bussmann-Holder A and Keller H 2005 *Eur. Phys. J.* B **44** 487

[56] Bussmann-Holder A and Keller H 2007 *Polarons in Advanced Materials* (*Springer Series in Materials Science*) vol 103, ed A S Alexandrov (Heidelberg: Springer) p 599

[57] Furrer A 2005 *Superconductivity in Complex Systems* (*Springer Series Structure and Bonding* vol 114) ed K A Müller and A Bussmann-Holder (Heidelberg: Springer) p 171

[58] Bianconi A and Saini N L 2005 *Superconductivity in Complex Systems* (*Springer Series Structure and Bonding* vol 114) ed K A Müller and A Bussmann-Holder (Heidelberg: Springer) p 287

[59] Lanzara A, Zhao G M, Saini N L, Bianconi A, Conder K, Keller H and Müller K A 1999 *J. Phys.: Condens. Matter.* **11** L541

[60] Bussmann-Holder A 2000 *J. Supercond.* **13** 773

[61] Kamimura H, Hamada T, Matsuno S and Ushio H 2002 *J. Supercond.* **15** 379

[62] Boeri L, Dolgov O V and Golubov A A 2008 *Phys. Rev. Lett.* **101** 026403

[63] Mittal R, Su Y, Rols S, Tegel M, Chaplot S L, Schober H, Chatterji T, Johrendt D and Brueckel Th 2008 *Phys. Rev.* B **78** 224518
Mittal R, Su Y, Rols S, Chatterji T, Chaplot S L, Schober H, Rotter M, Johrendt D and Brueckel Th 2008 *Phys. Rev.* B **78** 104514

[64] Higashitaniguchi S 2008 *Phys. Rev.* B **78** 174507

[65] Lee P A and Wen X G 2008 *Phys. Rev.* B **78** 114517
Day X, Fang Z, Zhou Y and Zhang F-C 2008 *Phys. Rev. Lett.* **101** 057008
Han Q, Chen Y and Wang Z D 2008 *Europhys. Lett.* **82** 37007

[66] Barzykin V and Gorkov L P 2008 *JETP Lett.* **88** 131

[67] Zbiri M, Schober H, Johnson Mark R, Rols S, Mittal R, Su Yixi, Rotter M and Johrendt D 2009 *Phys. Rev.* B **79** 064511

[68] Mizuguchi Y, Hara Y, Deguchi K, Tsuda S, Yamaguchi T, Takeda K, Kotegawa H, Tou H and Takano Y 2010 *Supercond. Sci. Technol.* **23** 054013

[69] Granath M, Bielecki J, Holmlund J and Börjesson L 2009 *Phys. Rev.* B **79** 235103

[70] Shirage P M, Miyazawa K, Kihou K, Kito H, Yoshida Y, Tanaka Y, Eisaki H and Iyo A 2010 *Phys. Rev. Lett.* **105** 037004

[71] Khasanov R, Bendele M, Bussmann-Holder A and Keller H 2010 *Phys. Rev.* B **82** 212505

[72] Tsuei C C and Kirtley J R 2000 *Rev. Mod. Phys.* **72** 969

[73] Kirtley J R, Tsuei C C, Ariando , Verwijs C J M, Harkema S and Hilgenkamp H 2006 *Nature Phys.* **2** 190

[74] Friedl B, Thomsen C and Cardona M 1990 *Phys. Rev. Lett.* **65** 915

[75] Müller K A 2002 *Phil. Mag. Lett.* **82** 279
Müller K A 2007 *Handbook of High Temperature Superconductivity, Theory and Experiment* ed J R Schrieffer and J S Brooks (Berlin: Springer)

[76] Müller K A 1995 *Nature* **377** 133

[77] Müller K A and Keller H 1997 *High T_c Superconductivity: 10 Years After the Discovery* (Dordrecht: Kluwer) p 7

[78] Khasanov R, Shengelaya A, Maisuradze A, La Mattina F, Bussmann-Holder A, Keller H and Müller K A 2007 *Phys. Rev. Lett.* **98** 057007

[79] Khasanov R, Strässle S, Di Castro D, Masui T, Miyasaka S, Tajima S, Bussmann-Holder A and Keller H 2007 *Phys. Rev. Lett.* **99** 237601

[80] Khasanov R, Shengelaya A, Karpinski J, Bussmann-Holder A, Keller H and Müller K A 2008 *J. Supercond. Nov. Magn.* **21** 81

[81] Bussmann-Holder A, Khasanov R, Shengelaya A, Maisuradze A, La Mattina F, Keller H and Müller K A 2007 *Europhys. Lett.* **77** 27002

[82] Khasanov R, Shengelaya A, Bussmann-Holder A and Keller H 2007 *High T_c Superconductors and Related Transition Metal Oxides* ed A Bussmann-Holder and H Keller (Berlin: Springer) p 177

[83] Micnas R, Robaszkiewicz S and Bussmann-Holder A 2005 *Superconductivity in Complex Systems* (*Springer Series Structure and Bonding* vol 114) ed K A Müller and A Bussmann-Holder (Heidelberg: Springer) p 13

[84] Bussmann-Holder A and Keller H 2008 *J. Phys.: Conf. Ser.* **108** 012019

[85] Kohen A, Leibowitch G and Deutscher G 2003 *Phys. Rev. Lett.* **90** 207005

[86] Gonnelli R S, Daghero D, Tortello M, Ummarino G A, Stepanov V A, Kremer R K, Kim J S, Zhigadlo N D and Karpinski J 2009 *Physica* C **469** 512

[87] Yates K A, Morrison K, Rodgers J A, Penny G B S, Bos J-W G, Attfield J P and Cohen L F 2009 *New J. Phys.* **11** 025015

[88] Daghero D, Tortello M, Gonnelli R S, Stepanov V A, Zhigadlo N D and Karpinski J 2009 *Phys. Rev.* B **80** 060502 (R)

[89] Ponomarev Ya G *et al* 2009 *Phys. Rev.* B **79** 224517

[90] Nakayama K *et al* 2009 *Europhys. Lett.* **85** 67002

[91] Ding H *et al* 2008 *Europhys. Lett.* **83** 47001

[92] Evtushinsky D V *et al* 2009 *New J. Phys.* **11** 055069

[93] Li G, Hu W Z, Dong J, Li Z, Zheng P, Chen G F, Luo J L and Wang N L 2008 *Phys. Rev. Lett.* **101** 107004

[94] Gang Mu *et al* 2008 arXiv:0808.2941

[95] Khasanov R *et al* 2009 *Phys. Rev. Lett.* **102** 187005

[96] Szabó P, Pribulová Z, Pristáš G, Bud'ko S L, Canfield P C and Samuely P 2009 *Phys. Rev.* B **79** 012503

[97] Ren C, Wang Z-S, Luo H-Q, Yang H, Shan L and Wen H-H 2008 *Phys. Rev. Lett.* **101** 257006

[98] Khasanov R *et al* 2008 *Phys. Rev.* B **78** 220510 (R)

[99] Dong J K, Guan T Y, Zhou S Y, Qiu X, Ding L, Zhang C, Patel U, Xiao Z L and Li S 2009 *Phys. Rev.* B **80** 024518

[100] Han G, Chen Y and Wang Z D 2008 *Europhys. Lett.* **82** 37007

[101] Zhao J *et al* 2008 *Nature Mater.* **7** 953

[102] Lebègue S 2007 *Phys. Rev.* B **75** 035110

[103] Horigane K, Hiraka H and Ohoyama K 2009 *J. Phys. Soc. Japan* **78** 074718

[104] Bussmann-Holder A, Simon A, Keller H and Bishop A R 2011 *J. Supercond. Nov. Magn.* **24** 1099

[105] Khasanov R, Strässle S, Conder K, Pomjakushina E, Bussmann-Holder A and Keller H 2008 *Phys. Rev.* B **77** 104530